SPE 112873

Efficient Ensemble-Based Closed-Loop Production Optimization

Yan Chen, Dean S. Oliver, SPE, University of Oklahoma and Dongxiao Zhang, SPE, University of Southern California

This paper was prepared for presentation at the 2008 SPE Improved Oil Recovery Symposium held in Tulsa, Oklahoma, U.S.A., 19-23 April 2008.

Abstract

With the advances in smart well technology, substantially higher oil recovery can be achieved by intelligently managing the operations in a closed-loop optimization framework. The closed-loop optimization consists of two parts: geological model updating and production optimization. Both of these parts require gradient information to minimize or maximize an objective function: squared data mismatch or the net present value (or other quantities depending on financial goals), respectively. Alternatively, an ensemble-based method can acquire the gradient information through the correlations provided by the ensemble. Computation of the optimal controls in this way is nearly independent of the number of control variables, reservoir simulator and simulation solver. In this paper, we propose an ensemble-based closed-loop optimization method that combines a novel ensemble-based optimization scheme (EnOpt) with the ensemble Kalman filter (EnKF). The EnKF has recently been found suitable for sequential data assimilation in large-scale nonlinear dynamics. It adjusts reservoir model variables to honor observations and propagates uncertainty in time. The EnOpt optimizes the expectation of the net present value based on the updated reservoir models. The proposed method is fairly robust, completely adjoint-free and can be readily used with any reservoir simulator. The ensemble-based closed-loop optimization method is illustrated with a waterflood example subject to uncertain reservoir description. Results are compared with other possible reservoir operation scenarios, such as, wells with no controls, reactive control, and optimization with known geology. The comparison shows that the ensemble-based closed-loop optimization is able to history match the main geological features and increase the net present value to a level comparable with the hypothetical case of optimizing based on known geology.

Introduction

Production optimization offers the potential to substantially increase ultimate oil recovery by developing an improved operating plan for a particular reservoir of interest. Since the economic objective involves evaluations of future achievements, it requires a reservoir simulation model for prediction and is usually referred to as a model-based optimization technique. Due to limited access to the reservoir, the reservoir geological model is subject to high uncertainty. In order to obtain a suitable production strategy for the reservoir of interest, production optimization needs to be combined with a parameter estimation method that reduces the uncertainty of the estimate of the reservoir geological properties. Closed-loop optimization (Brouwer et al., 2004; Sarma et al., 2005b; Wang et al., 2007) combines production optimization with data assimilation to form a real time reservoir management. Data assimilation is a sequential model updating method, where the estimate of the uncertain parameters is updated continuously to be consistent with the production data available in time. The workflow of the closed-loop optimization technique is typically as follows (see Fig. 1). An initial geological model is built using available prior knowledge of the reservoir and the initial production strategy is chosen based on this prior knowledge. At times when production data are available, the reservoir geological model is updated, and the updated geological model provides the basis for a better estimate of the true reservoir behavior. The production strategy is then optimized based on the newly updated reservoir model. This process can be carried out in real time, and the management of the reservoir is kept up-to-date.

Both model updating and production optimization are optimization problems. Model updating aims at minimizing the mismatch between the model predictions and the historical production data. It is commonly known as

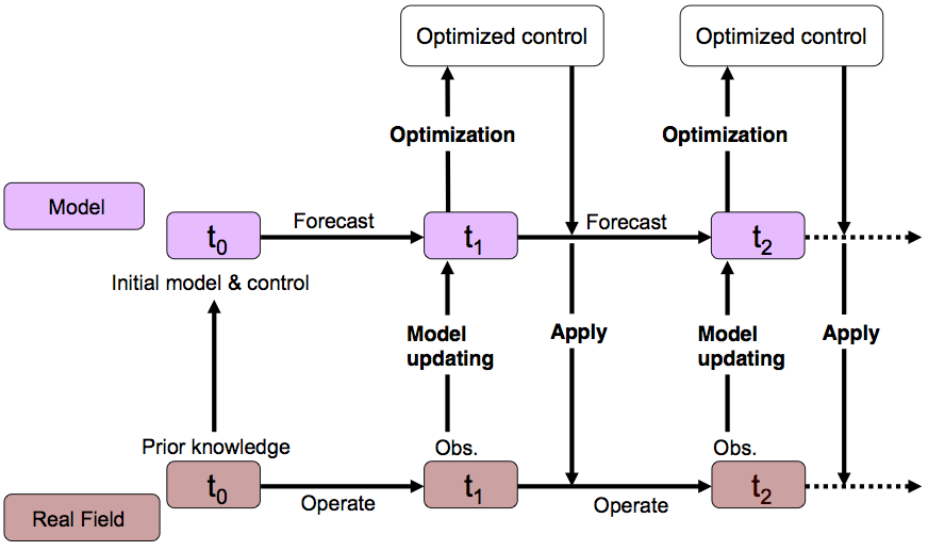

Figure 1: The flowchart for closed-loop optimization.

history matching in petroleum reservoir applications. Production optimization aims at maximizing the net present value (NPV) or other quantities depending on financial goals. Gradient-based approaches are commonly used to solve optimization problems. Since multiphase flow and transport problems are nonlinear, the gradient-based method is usually carried out in an iterative form. A series of linearizations (iterations) are performed in the search for a minimum, and at each iteration a gradient is needed to determine the search direction. Various gradient calculation methods including numerical perturbation, sensitivity equation and adjoint method have been developed. The numerical perturbation method (finite difference approximation) is straightforward to implement but the computation involved is proportional to the number of unknown parameters. The number of unknown parameters of the geological model is usually large, two or more parameters per gridblock, although for some problems it may be possible to reduce the number of parameters describing important aspects of the model (Van Doren et al., 2008). For the production optimization, controls of wells (well constraints) are the unknowns and the number of control variables is proportional to the number of wells and the number of times at which the control variables are changed. The numerical perturbation method becomes extremely expensive when the number of unknown parameters is large. Computation of gradients from the adjoint method is independent of the number of unknowns, but requires access to the simulator source code and substantial code development. Li et al. (2003) pointed out that the coefficient matrix of the adjoint equations is simply the transpose of the Jacobian matrix used in a fully implicit reservoir simulator. By extracting and saving the Jacobian matrices, the process of deriving individual adjoint equation can be avoided. Sarma et al. (2005a) used similar idea and developed a modified adjoint method for production optimization. But the use of this modified optimization method requires a fully implicit reservoir simulator, a specific form of the objective function and considerable data storage.

Alternatively, an ensemble-based method can be used to compute an approximation to the gradient through the sensitivity provided by the ensemble, and the simulator only serves as a black box. Approximating the sensitivity from the ensemble gives us great flexibility of using different reservoir simulators and simulation solvers. Sensitivity can be easily computed by processing the inputs and outputs of all the ensemble runs and the computational cost is nearly independent of the number of unknown parameters. One of the ensemble-based methods, the ensemble Kalman filter (EnKF), has attracted great research interests since the original work of Evensen (1994). The EnKF has been found suitable for sequential data assimilation in large-scale nonlinear dynamics (Houtekamer and Mitchell, 2001; Mitchell et al., 2002; Bertino et al., 2003). Specifically, it has been shown to be suitable for history matching problem with possible modifications (Nævdal et al., 2005; Gu and Oliver, 2005; Liu and Oliver, 2005; Haugen et al., 2006; Chen et al., 2007; Li and Reynolds, 2007; Gu and Oliver, 2007). The EnKF utilizes the ensemble-based sensitivity to adjust an ensemble of geological models to be consistent with the observed production data. By keeping track of the entire ensemble, the EnKF is able to provide both the estimate of the geological model and the corresponding uncertainty.

In the literature, various methods of history matching and production optimization have been combined together to form the closed-loop optimization framework. Brouwer et al. (2004) used an adjoint method for optimization and the EnKF for model updating. Sarma et al. (2005b) used an adjoint method for both the model updating

and the production optimization. Karhunen-Loeve decomposition was used to represent the permeability field to reduce the number of unknown parameters and to preserve two-point geostatistics. Polynomial chaos expansions were used to propagate the uncertainty. Wang et al. (2007) combined the EnKF with three optimization methods using a small reservoir model. They concluded, based on their computational experiments, that the steepest ascent method with gradients provided by numerical perturbation gave better results than those with gradients provided by either an ensemble or simultaneous perturbation stochastic approximation.

In this paper, we propose an ensemble-based closed-loop optimization method that combines an ensemble-based optimization scheme (EnOpt) with the EnKF. Compared to the existing optimization methods, the EnOpt has two distinct features. First, the search direction used in the production optimization is approximated by an ensemble. Lorentzen et al. (2006) directly adopted the EnKF method to optimize choke settings. They utilized the sensitivity approximated by the ensemble but did not make the process clear and the use of a preset upper limit might need more justification. Second, the EnOpt aims at maximizing the expectation of the net present value instead of maximizing the net present value based on a single reservoir model, which is usually chosen to be the mean or the central model (Brouwer et al., 2004; Sarma et al., 2005a; Wang et al., 2007). By taking into account the uncertainty of the estimated geological model (provided by the EnKF) and optimizing the expectation of the net present value, the EnOpt is fairly robust with respect to the uncertain reservoir description.

In the remainder of the paper, we first briefly review the EnKF method, and then introduce the detailed formulation of the EnOpt and the procedure of the ensemble-based closed-loop optimization method. Two synthetic test problems are shown. The first test problem is to optimize production and injection rates for a channelized reservoir. In this example only the EnOpt is tested and the geological properties of the reservoir are assumed to be known. The ensemble-based closed-loop optimization is illustrated by the second example. The reservoir permeability is considered to be the only uncertain parameter and is updated using the EnKF. The EnOpt is used to optimize the well control settings based on the continuously updated geological model. Results of the closed-loop optimization are compared with those obtained from other possible reservoir operation scenarios, such as, wells with no controls, reactive control (model free), and optimization with known geology. The comparison shows that the closed-loop optimization is able to adjust the geological model to reflect the true feature of the reservoir and to achieve considerable increase of the NPV upon optimization. The level of increase of the NPV is comparable with the hypothetical case of optimization with known geology.

Methodology

Ensemble Kalman filter (EnKF) The formulation of the EnKF has been well documented in Evensen (2003); Nævdal et al. (2005) and Chen and Zhang (2006). Only a brief outline is given here in order to show the connection between the EnKF and the EnOpt. In the EnKF, we collect all the variables of interest into a state vector $\mathbf{y}$. We refer to these variables as state variables. A typical state vector of a two-phase flow problem is composed of porosity, permeability, pressure and water saturation at each gridblock and all the available production data

$$\mathbf{y} = [\boldsymbol{\phi},\, \ln \boldsymbol{k},\, \mathbf{P},\, \mathbf{S_w},\, \mathbf{WPR},\, \mathbf{OPR}]^T \,. \tag{1}$$

Vector notation is used for the components of $\mathbf{y}$, because they are vectors containing either the static or dynamic variables at all the gridblocks or production data from all the wells. For the EnKF application, an ensemble of state vectors are collected in a matrix $\mathbf{Y}$

$$\mathbf{Y} = [\mathbf{y}_1,\, \mathbf{y}_2,\, \mathbf{y}_3,\, \ldots,\, \mathbf{y}_{N_e}] \,, \tag{2}$$

where N_e is the total number of the ensemble members. The statistics needed for the updating step are approximated from the ensemble. At the updating step, each ensemble member is updated using

$$\mathbf{y}_j^{\mathrm{u}} = \mathbf{y}_j^{\mathrm{f}} + \mathbf{C_Y H}^T(\mathbf{H C_Y H}^T + \mathbf{C_D})^{-1}(\mathbf{d_{obs},}_j - \mathbf{H}\mathbf{y}_j^{\mathrm{f}}), \quad j = 1, 2, \ldots, N_e \,, \tag{3}$$

where j is the index of the individual ensemble member and $\mathbf{d_{obs},}_j$ is the perturbed observation in order to maintain the correct variance after updating (Burgers et al., 1998). The superscript "u" indicates update and superscript "f" indicates forecast. $\mathbf{C_D}$ is the covariance matrix of the measurement noise. $\mathbf{H}$ is a matrix operator that selects measured variables from the state vector. The product $\mathbf{C_Y H}$ is the cross-covariance between all the state variables and the predicted observations and $\mathbf{H C_Y H}$ is the auto-covariance of the predicted observations. The covariance of the state vector is approximated using the standard statistical formula as

$$\mathbf{C_Y} \approx \frac{1}{N_e - 1}(\mathbf{Y}^{\mathrm{f}} - \langle \mathbf{Y}^{\mathrm{f}} \rangle)(\mathbf{Y}^{\mathrm{f}} - \langle \mathbf{Y}^{\mathrm{f}} \rangle)^T \,, \tag{4}$$

where $\langle \mathbf{Y}^{\mathrm{f}} \rangle$ denotes the mean of the state vector.

Ensemble-based optimization (EnOpt) We use $\mathbf{x}$ to represent the vector of control variables that contains all the well constraints at different control steps,

$$\mathbf{x} = [x_1,\, x_2,\, x_3,\, \ldots,\, x_{N_x}]\,, \tag{5}$$

where N_x is the total number of the control variables, and it is equal to the product of the number of wells and the number of control steps. The components of $\mathbf{x}$ first cycle through the control steps for a single well then cycle through all the wells. In this study the objective of the ensemble-based optimization (EnOpt) is to maximize the net present value of the reservoir, but the algorithm of the EnOpt is not limited to the form of the objective function, as we will see in this subsection. The calculation of the net present value is given as

$$g(\mathbf{x},\mathbf{y}) = \sum_{i=1}^{N_t} \frac{v_{\mathrm{o}} Q_{\mathrm{o}_i}(\mathbf{x},\mathbf{y}) - v_w Q_{\mathrm{w}_i}(\mathbf{x},\mathbf{y})}{(1+r_\tau)^{t_i/\tau}}\,, \tag{6}$$

where i is the time step index; N_t is the total number of time steps; r_τ is the discount rate in terms of time span τ and t_i is the accumulative time since the start of production. v_{o} and v_{w} are the price of oil and the cost of water disposal, respectively. Q_{o_i} and Q_{w_i} are the total oil and water production over time step Δt_i. $\mathbf{y}$ indicates the reservoir properties (Eq. 1) and $\mathbf{x}$ indicates the control variables (Eq. 5). Q_{o_i} and Q_{w_i} depend on both the reservoir properties and the control variables, thus the net present value $g(\mathbf{x},\mathbf{y})$ is expressed as a function of both $\mathbf{x}$ and $\mathbf{y}$.

In the EnOpt, the control variables are optimized under the consideration of the uncertainty of the reservoir model. We use the expectation of the net present value over this uncertain description of the reservoir geological properties as the objective function to take into account the uncertainty of the reservoir model. Since this uncertainty is represented by the ensemble propagated by the EnKF, the objective function becomes

$$g_{\mathbf{Y}}(\mathbf{x}) = \frac{1}{N_e}\sum_{j=1}^{N_e} g(\mathbf{x},\mathbf{y}_j)\,. \tag{7}$$

The subscript $\mathbf{Y}$ of $g_{\mathbf{Y}}(\mathbf{x})$ indicates that the value of $g_{\mathbf{Y}}(\mathbf{x})$ depends on the pdf of the reservoir models updated in the EnKF. Because the ensemble $\mathbf{Y}$ is not modified during the production optimization, $g_{\mathbf{Y}}(\mathbf{x})$ is considered as a function of control variables $\mathbf{x}$ only. To simply the notation, however, the subscript $\mathbf{Y}$ is suppressed in the remaining of this section.

We utilize the steepest ascent method to seek control variables $\mathbf{x}$ that maximize the objective function $g(\mathbf{x})$. The steepest ascent method is formulated as

$$\mathbf{x}_{\ell+1} = \frac{1}{\alpha_\ell}\mathbf{C}_{\mathbf{x}}\mathbf{G}_\ell^T + \mathbf{x}_\ell\,, \tag{8}$$

where ℓ denotes the iteration index, α_ℓ is a tuning parameter that determines the step size in the steepest ascent direction, $\mathbf{G}_\ell$ is the sensitivity of $g(\mathbf{x})$ to the control variables evaluated at the ℓth iteration and $\mathbf{C}_{\mathbf{x}}$ is the prior covariance matrix of the control variables $\mathbf{x}$. The use of the covariance matrix $\mathbf{C}_{\mathbf{x}}$ in front of the sensitivity matrix provides a preconditioning for the steepest ascent method (Tarantola, 2005). In this particular case we choose the Gaussian covariance function to specify the temporal correlation of the controls at each well, and suppose the controls of different wells are uncorrelated. Thus $\mathbf{C}_{\mathbf{x}}$ is a block matrix with Gaussian covariance matrices on the diagonal and zero matrices for the off-diagonal elements. The choice of a Gaussian covariance matrix comes from a desire to limit the frequency and magnitude of changes in the well controls. Although we assumed that the control variables are uncorrelated among different wells, there are some production constraints which could bring in dependency among different wells. Commonly used ones are the total water injection rate and the total fluid production rate. Additionally, there are always upper and lower limits for different control parameters depending on the capacity of the facilities, for example the minimum and maximum bottom hole pressures and the minimum and maximum surface production and injection rates. In this study, constraints are handled simplistically. The values which are outside the bounds are truncated and the total rate constraint is honored by reallocating the rates among wells proportionally according to the truncated values.

In order to approximate the sensitivity of $g(\mathbf{x})$ to the control variables $\mathbf{x}$, $\mathbf{G}_\ell$, we form another ensemble $\hat{\mathbf{Y}}$

$$\begin{aligned}\hat{\mathbf{Y}} &= [\hat{\mathbf{y}}_1,\, \hat{\mathbf{y}}_2,\, \hat{\mathbf{y}}_3,\, \ldots,\, \hat{\mathbf{y}}_{N_e}] \\ &= \begin{bmatrix} \mathbf{x}_{\ell,1} & \mathbf{x}_{\ell,2} & \mathbf{x}_{\ell,3} & \cdots & \mathbf{x}_{\ell,N_e} \\ g(\mathbf{x}_{\ell,1},\mathbf{y}_1) & g(\mathbf{x}_{\ell,2},\mathbf{y}_2) & g(\mathbf{x}_{\ell,3},\mathbf{y}_3) & \cdots & g(\mathbf{x}_{\ell,N_e},\mathbf{y}_{N_e}) \end{bmatrix}.\end{aligned} \tag{9}$$

The ensemble $\hat{\mathbf{Y}}$ contains N_e realizations of $\hat{\mathbf{y}}_j$, where $j = 1, 2, 3, \ldots, N_e$. The size of the $\hat{\mathbf{Y}}$ ensemble is taken to be the same as the one used in the EnKF, but not necessarily. $\mathbf{x}_{\ell,j}$ are realizations of the control variables and each of them includes all the well constraints at each control step as shown in Eq. 5. These realizations of control variables are generated by perturbing the control variables $\mathbf{x}_\ell$ at the current iteration with temporally correlated Gaussian random variables. The presence of the second sub index differentiates them from the control variables $\mathbf{x}_\ell$ in Eq. 8. Note that forming an ensemble of the control variables is merely a way of approximating the product $\mathbf{C_x}\mathbf{G}_\ell^T$, and only $\mathbf{x}_\ell$ is updated in Eq. 8. $\mathbf{y}_j$ are the geological models propagated in the EnKF. The evaluation of $g(\mathbf{x}_{\ell,1}, \mathbf{y}_1)$, $g(\mathbf{x}_{\ell,2}, \mathbf{y}_2)$, $g(\mathbf{x}_{\ell,3}, \mathbf{y}_3)$, ..., $g(\mathbf{x}_{\ell,N_e}, \mathbf{y}_{N_e})$ couples the control realizations with the ensemble of geological models. Basically, we apply one realization of the control variables $\mathbf{x}_{\ell,j}$ to one geological model $\mathbf{y}_j$. The $g(\mathbf{x}_{\ell,j}, \mathbf{y}_j)$ are then calculated based on the simulation results using Eq. 6. The construction of the state vectors $\hat{\mathbf{Y}}$ thus involves N_e simulation runs. The realizations of the reservoir model reflect the uncertainty of the estimation of the geological properties. By coupling the control realizations with this ensemble of geological models, The EnOpt is able to take into account the uncertainty of the estimate of the reservoir geological properties and optimize the expectation of the net present value over the uncertain reservoir description.

We denote the cross-covariance between the control variables and $g(\mathbf{x})$ by $\mathbf{C}_{\mathbf{x},g(\mathbf{x})}$, and approximate it from the ensemble using

$$\mathbf{C}_{\mathbf{x},g(\mathbf{x})} \approx \frac{1}{N_e - 1} \sum_{j=1}^{N_e} \Big(\mathbf{x}_{\ell,j} - \langle \mathbf{x}_\ell \rangle \Big) \Big(g(\mathbf{x}_{\ell,j}, \mathbf{y}_j) - \langle g(\mathbf{x}_\ell, \mathbf{y}) \rangle \Big) , \tag{10}$$

where

$$\begin{aligned} \langle \mathbf{x}_\ell \rangle &= \frac{1}{N_e} \sum_{j=1}^{N_e} \mathbf{x}_{\ell,j} , \\ \langle g(\mathbf{x}_\ell, \mathbf{y}) \rangle &= \frac{1}{N_e} \sum_{j=1}^{N_e} g(\mathbf{x}_{\ell,j}, \mathbf{y}_j) . \end{aligned} \tag{11}$$

Since $\mathbf{x}_{\ell,j}, j = 1, 2, 3 \ldots N_e$ were generated by perturbing $\mathbf{x}_\ell$ with zero mean correlated Gaussian random variables, we have $\langle \mathbf{x}_\ell \rangle \approx \mathbf{x}_\ell$. Suppose at each iteration, $g(\mathbf{x}, \mathbf{y})$ is linearized at $\mathbf{x}_\ell$ as $g(\mathbf{x}, \mathbf{y}) \approx g(\mathbf{x}_\ell, \mathbf{y}) + \mathbf{G}_\ell(\mathbf{x} - \mathbf{x}_\ell)$ and $\langle g(\mathbf{x}_\ell, \mathbf{y}) \rangle \approx g(\langle \mathbf{x}_\ell \rangle, \mathbf{y}) \approx g(\mathbf{x}_\ell, \mathbf{y})$, so the product of $\mathbf{C_x}\mathbf{G}_\ell^T$ can be approximated by

$$\mathbf{C}_{\mathbf{x},g(\mathbf{x})} \approx \mathbf{C_x}\mathbf{G}_\ell^T . \tag{12}$$

Because the cross-covariance is estimated using the Monte Carlo method (Eq. 10), the estimation might suffer from the spurious correlation when the size of the ensemble is small. A similar situation occurs in the estimation of $\mathbf{C_Y}$ in Eq. 4. Usually localization is used to reduce the effect of the spurious correlation in the application of the EnKF (Hamill and Whitaker, 2001; Arroyo-Negrete et al., 2006; Agbalaka and Oliver, 2007). In the EnKF the localization is done by filtering out the cross-covariance beyond a critical distance (localization was not used in the data assimilation in this paper). In the production optimization, the unknowns are the well constraints at different control steps, and the range of the filtering matrix is the time period within which we trust the ensemble-based sensitivity. Because the variance is not important in the control optimization, we used a standard matrix product (not the Schur product) of the covariance matrix of the control variables $\mathbf{C_x}$ for localization and conditioning.

After substituting Eq. 12 in Eq. 8 and using $\mathbf{C_x}$ as a filtering (smoothing) matrix, the steepest ascent method used in the EnOpt becomes

$$\mathbf{x}_{\ell+1} = \frac{1}{\alpha} \mathbf{C_x} \mathbf{C}_{\mathbf{x},g(\mathbf{x})} + \mathbf{x}_\ell . \tag{13}$$

Another interpretation is by premultiplying $\mathbf{C}_{\mathbf{x},g(\mathbf{x})}$ by $\mathbf{C_x}$ we restore the smoothness lost in approximating the $\mathbf{C}_{\mathbf{x},g(\mathbf{x})}$ by a small-sized ensemble. We denote the square of the covariance matrix $\mathbf{C_x}$ by $\mathbf{R_x}$. The square of a Gaussian covariance matrix is also a Gaussian covariance matrix with larger range (Oliver, 1995). Eq. 13 changes to

$$\begin{aligned} \mathbf{x}_{\ell+1} &= \frac{1}{\alpha} \mathbf{C_x} \mathbf{C}_{\mathbf{x},g(\mathbf{x})} + \mathbf{x}_\ell \\ &= \frac{1}{\alpha} \mathbf{C_x} \mathbf{C_x} \mathbf{G}_\ell^T + \mathbf{x}_\ell \\ &= \frac{1}{\alpha_\ell} \mathbf{R_x} \mathbf{G}_\ell^T + \mathbf{x}_\ell , \end{aligned} \tag{14}$$

which is the original steepest ascent equation (Eq. 8) with $\mathbf{R}_\mathbf{x}$ as the preconditioner.

Several previous studies also attempted to compute the gradient of the expected net present value with respect to the control variables. Sarma et al. (2005b) used the adjoint method to compute the expectation of the NPV with respect to the controls, and the uncertainty of the reservoir description is propagated using the probability collocation method (PCM). van Essen et al. (2006) also considered using the expectation of the NPV as the objective function. They used an ensemble of reservoir models to reflect the uncertainty of the geological model and solved the adjoint equations for each realization. The average of the resulting gradients is considered as the gradient of the expected NPV with respect to the controls. Both of the methods require the availability of the adjoint code. Compared to these two methods, The EnOpt simply approximates the average sensitivity of the expected NPV to the control variables from the coupled ensemble of controls and ensemble of geological models. It is fairly flexible in terms of the choice of the controls variables and the choice of the objective function to be optimized, and there is no limitation of using existing complicated well models available in various reservoir simulators.

Implementation of ensemble-based closed-loop optimization The procedure of the ensemble-based closed-loop optimization is summarized in this subsection. Note that k is the index for data times; $\mathbf{Y}_k, k = 1, 2, \ldots, N_D$ are ensembles of geological models updated at different data times; $\mathbf{x}$ is the vector of control variables. ℓ is the iteration index of the EnOpt; $\mathbf{x}_\ell$ is the control variables at the ℓth iteration and $\mathbf{x}_{\ell,j}, j = 1, 2, \ldots, N_e$ are realizations of control variables used to approximate $\mathbf{C}_\mathbf{x}\mathbf{G}_\ell^T$.

INITIALIZATION: EnKF

1. let $k = 0$, and generate the initial ensemble $\mathbf{Y}_0$ based on the prior knowledge. The initial control variables $\mathbf{x}$ are also chosen based on the prior knowledge.

START OF LOOP: EnKF

2. Integrate ensemble $\mathbf{Y}_k$ with true well constraints $\mathbf{x}$ from the current data time t_k to the next data time t_{k+1} using the reservoir simulator.

3. At t_{k+1}, update $\mathbf{Y}_k$ by incorporating the observed production data using Eq. 3 and let $k = k + 1$.

INITIALIZATION: EnOpt

4. Let $\ell = 1$. Generate initial control variables $\mathbf{x}_1$ and initial ensemble of control variables $\mathbf{x}_{1,j}, j = 1, 2, \ldots N_e$.

   - If $k = 1$, $\mathbf{x}_{1,j}$ are generated in two steps. First, a mean control is sampled from a uniform distribution with the upper and lower limits equal to the maximum and minimum possible well constraints for each realization of each well. Second, a temporally correlated Gaussian random field with zero mean is generated for each realization of each well and added to the mean control. Set $\mathbf{x}_1 = 1/N_e \sum_{j=1}^{N_e} \mathbf{x}_{1,j}$.
   - If $k \neq 1$, $\mathbf{x}_1$ is set equal to $\mathbf{x}$. A temporally correlated Gaussian random field with zero mean is generated for each realization of each well and added to the control variables $\mathbf{x}_1$ to form $\mathbf{x}_{1,j}$.

START OF LOOP: EnOpt based on ensemble $\mathbf{Y}_k$

5. If $\ell \neq 1$, a temporally correlated Gaussian random field with zero mean is generated for each realization of each well and added to the control variables $\mathbf{x}_\ell$.

6. Run the simulator from t_k to the end of the field life and compute $g(\mathbf{x}_{\ell,j}, \mathbf{y}_j)$ using the simulation results through Eq. 6, where $\mathbf{y}_j$ are members of the $\mathbf{Y}_k$ ensemble.

7. Compute the cross covariance $\mathbf{C}_{\mathbf{x},g(\mathbf{x})}$ using Eq. 10.

8. Compute the updated control variables $\mathbf{x}_{\ell+1}$ using Eq. 13.

9. Evaluate the objective function $g(\mathbf{x}_{\ell+1})$ using Eq. 7, which requires N_e simulation runs.

10. If $g(\mathbf{x}_{\ell+1}) > g(\mathbf{x}_\ell)$, overwrite $\mathbf{x}_\ell$ by $\mathbf{x}_{\ell+1}$ and let $\ell = \ell + 1$; otherwise keep $\mathbf{x}_\ell$, increase α_ℓ and go to step (8).

11. Check if the stopping criteria are satisfied. If not, go to step (5), otherwise set $\mathbf{x} = \mathbf{x}_\ell$ and exit the loop of EnOpt.

END OF LOOP: EnOpt based on ensemble $\mathbf{Y}_k$

12. If all data are assimilated, exit the loop of EnKF, otherwise go to step (2).

END OF LOOP: EnKF

Note that in step (1) the initial control variables are chosen based on the prior knowledge. If preferred, optimization could also be done on the initial ensemble to generate the initial control variables $\mathbf{x}$. The initial ensemble, however, usually is not a very good representation of the true reservoir and thus the optimized control variables using the initial ensemble might not be much better than naive controls. We delay optimization until after the first data assimilation to reduce the computation.

The stopping criteria used in step (11) are: (1) the relative increase of the objective function is less than 0.01%; (2) the change to the control variables in two consecutive iterations is less than 1%; (3) the number of increases of the tuning parameter α is greater than two.

In the case where the geological properties of the reservoir are assumed to be known the procedure is much simplified. The EnKF loop can be eliminated since the geological model is deterministic. All the $\mathbf{y}_j$ appearing in the EnOpt loop are equal to the known reservoir model $\mathbf{y}_{\text{ref}}$. Evaluation of the objective function, step (9), only requires a single simulation run to compute $g(\mathbf{x}_{\ell+1}, \mathbf{y}_{\text{ref}})$.

Illustrative examples

We will consider two synthetic examples in this section to demonstrate the performance of the proposed approach. The first example is a test of the ensemble-based optimization (EnOpt). The EnOpt is used to optimize injection and production rates to maximize the net present value (NPV) at a fixed time frame. A channelized reservoir is considered in this example, and the geological properties of the reservoir are assumed to be known. The second problem is an example of the ensemble-based closed-loop optimization, where the gridblock permeability is assumed to be uncertain. The underlying reference permeability field has a high permeability streak crossing through the reservoir in the main flow direction. The high permeability streak feature resembles the example considered in Brouwer et al. (2004) and Sarma et al. (2005a). The reservoir is completed with one horizontal injector and one horizontal producer, each of which has ten control valves installed. The degree of opening of the valves is the control parameter to be optimized.

Ensemble-based optimization We consider a two dimensional two-phase reservoir model in this section. The size of the reservoir is 2250×2250 ft^2. It is uniformly discretized into 45×45 square cells, each of size 50×50 ft^2. The net pay thickness is 30 ft. Only two different facies with uniform properties are present in the model. One is a channel sand with permeability equal to 8 D, and the other is a background shale with permeability equal to 10 mD. The permeability field (shown in Fig. 2) is assumed to be known. Porosity is assumed to be uniform throughout the reservoir and equal to 0.2. Nine producers and four injectors are completed in a repeated five spot pattern as shown in Fig. 2. The injectors are controlled by water injection rate and the producers are controlled by reservoir fluid volume rate target. Bottom hole pressure constraints are also imposed on the wells, being 500 psi for the producers and 8000 psi for the injectors. Additional constraints are total water injection rate of 4500 rb/day and total fluid production rate of 4500 rb/day. The price of oil is \$70/bbl and the cost of water disposal is \$5/bbl. The discount rate is 10% per year. The time frame for the NPV optimization is 1020 days and the control settings are modified every two months, so the number of control steps is 17. Thus the total number of control parameters is 221, which is the product of the number of the wells and the number of the control steps. 50 realizations of controls are used in this example.

Results and discussions In the base case used for comparison, the total water injection rate and the total fluid production target are equally distributed among the injectors and producers, so all the injectors are controlled by water injection rate of 1125 rb/day, and all the producers are controlled by reservoir fluid production target of 500 rb/day. In the optimized case, the constraints of the total water injection rate and the total fluid production rate are also imposed. The aim of the optimization is to redistribute these rate targets among all the wells in order to achieve higher NPV. Fig. 3 shows the change of the NPV with iterations used in the EnOpt, and the horizontal blue line indicates the NPV earned in the base case. 15 iterations are used in this example and the iteration is terminated due to the increase of the NPV less than 0.01%.

The cumulative oil and water production of the base case (blue) and the optimized case (red) are compared in Fig. 4. The major contribution of the optimization in this case is reducing water production while maintaining relatively high oil production by wisely distributing the injection and production targets. As shown in Fig. 4, the final cumulative oil production is slightly higher and the water production is much less in the optimized case than in the base case.

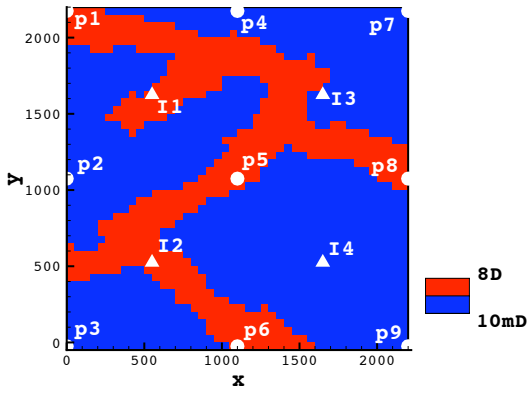

Figure 2: The permeability distribution of the channelized field and the location of the wells.

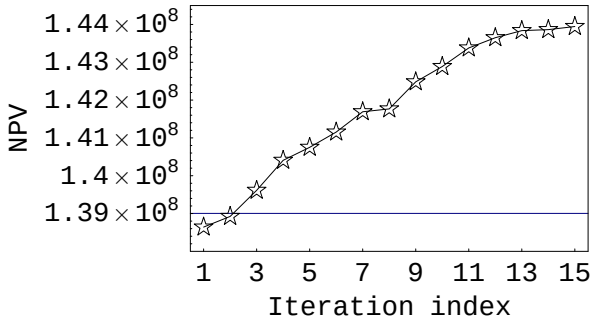

Figure 3: The change of the NPV with iterations used in the EnOpt. The blue line is the NPV earned by equally distributing injection and production rate among the wells (base case).

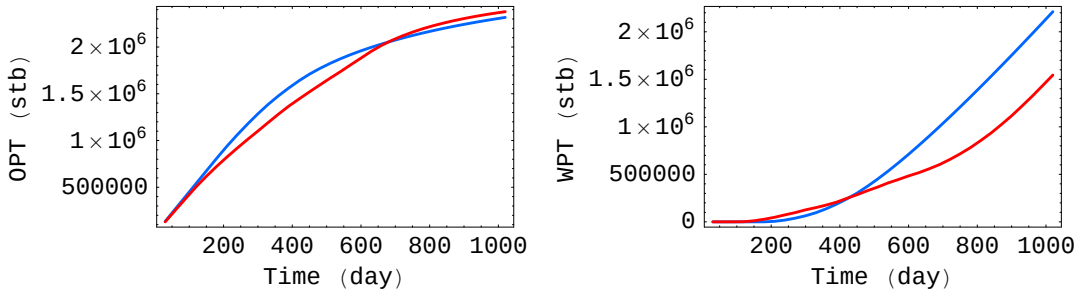

(a) Cumulative oil production

(b) Cumulative water production

Figure 4: Comparison of the cumulative oil and water production. Blue indicates the base case and red indicates the optimized case.

Fig. 5 shows the oil and water production rates from different producers for the base case and the optimized case. In the base case, all the producers behave similarly due to the same fluid production rate constraint imposed. In the optimized case the four producers located in the high permeability channel (p1, p5, p6, and p8) show much higher oil production initially. Although the higher oil production comes with the price of higher or earlier water production, in terms of the NPV it is still profitable. The oil production from the other five producers is delayed until later in the producing life, while the producers located in the high permeability channel at late time are all maintained under a very lower production rate to reduce the amount of producing water.

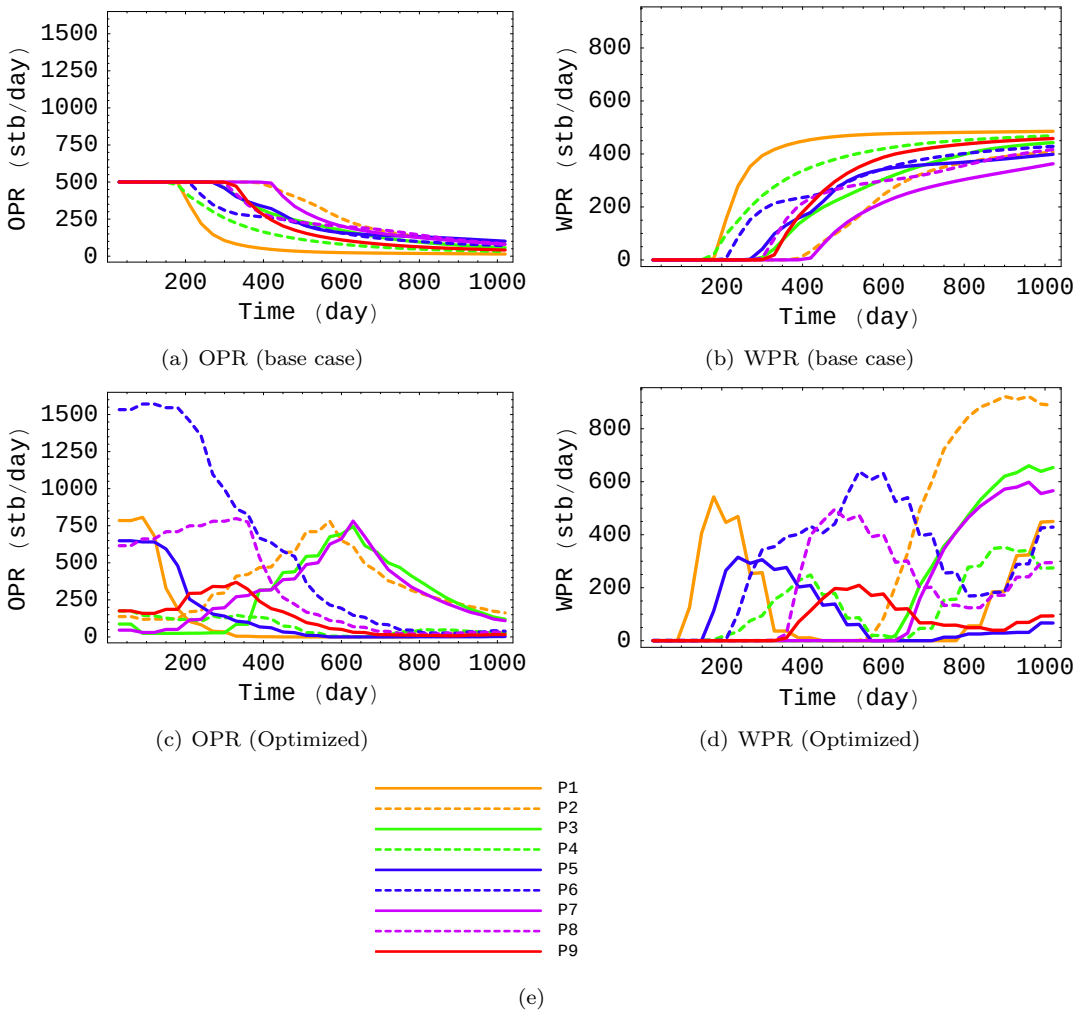

(a) OPR (base case)

(b) WPR (base case)

(c) OPR (Optimized)

(d) WPR (Optimized)

(e)

Figure 5: Comparison of the oil and water production from each producer between the base case and the optimized case.

Fig. 6 shows the change of the control variables $\mathbf{x}_\ell$ with iterations for several wells. The control settings at the first iteration is very close to those used in the base case and they are gradually improved by the EnOpt. The changes to the controls are relatively large at the early iterations, and the control settings tend to converge in the later iterations.

Summary In this example, the reservoir properties were assumed to be known without uncertainty and the well controls were optimized based on the true reservoir. The total water injection rate and the total fluid production rate were redistributed among the wells to maximize the NPV at the end of life of the reservoir. The major contribution of the optimization in this particular example was reducing water production and the NPV was increased by 3.6% from the base case. The amount of increase of the NPV and the optimized control settings depend on the choice of the parameters used in the calculation of the NPV. If the cost of the water disposal is much higher than the one used in this example, the optimized control setting shows more tendency to reduce water production and the percentage increase of the NPV is much higher compared to the current example due to larger benefit of the reduction of producing water.

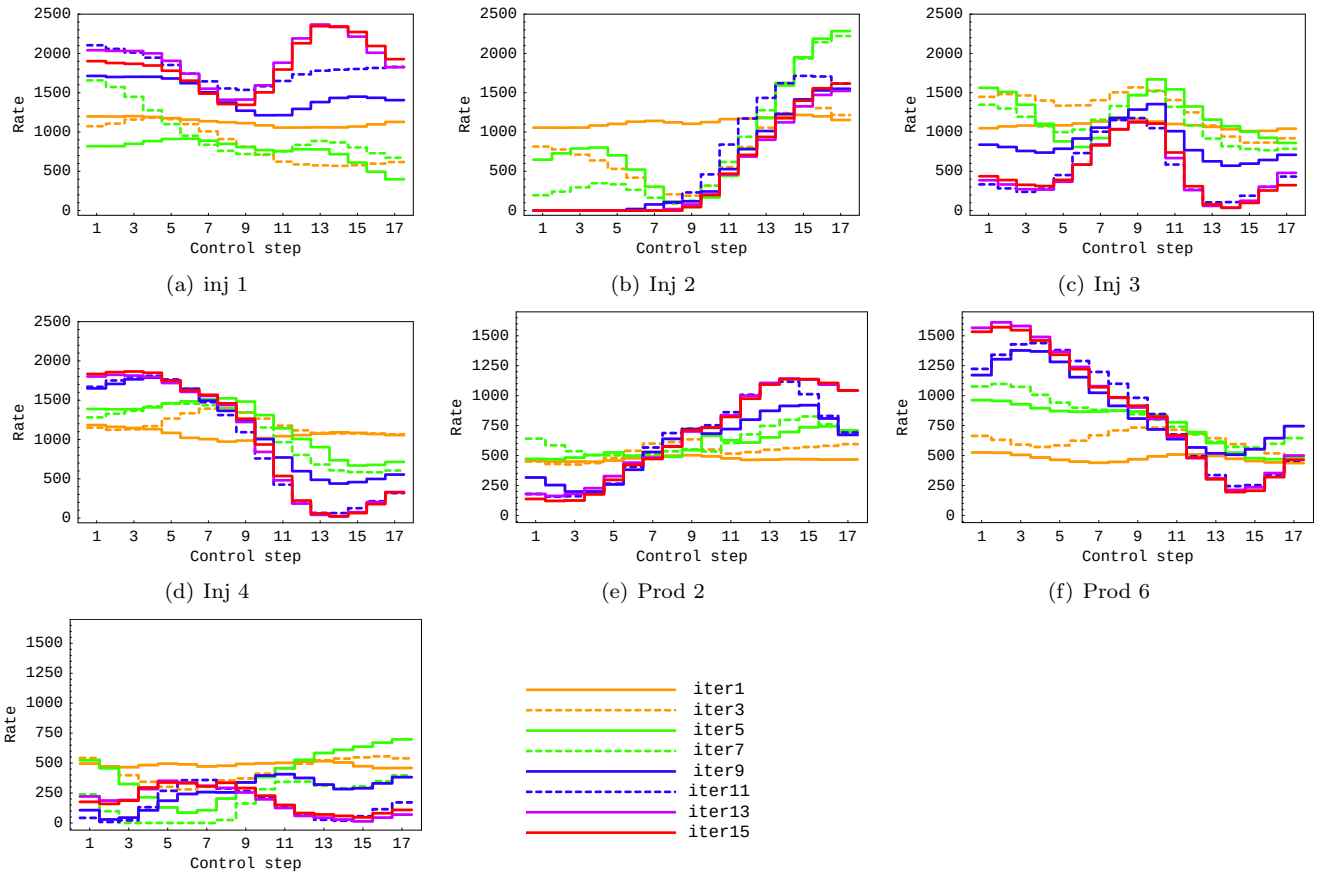

(a) inj 1 (b) Inj 2 (c) Inj 3

(d) Inj 4 (e) Prod 2 (f) Prod 6

(g) Prod 9 (h)

Figure 6: The change of the control settings with iterations.

This first example investigated the idealized situation in which there is no uncertainty in the geological properties; it will be referred to as optimization with known geology. Closed-loop optimization requires both the optimization of control variables and the estimation of properties of the reservoir model. Only the EnOpt is tested by this example where it showed reasonable results. The use of the EnOpt as an integral part of the ensemble-based closed-loop optimization will be examined in the next example.

Ensemble-based closed-loop optimization In this example we consider a reservoir of size 2050×2050 ft^2, uniformly discretized into 41×41 square cells. The net pay thickness is 40 ft. We assume only two phases, oil and water, are present. The irreducible water saturation and the residual oil saturation are both 0.2. Capillarity is neglected. Initially the reservoir is saturated with oil and irreducible water. We assume the north and the south sides are no-flow boundaries and permeability, which is to be estimated by incorporating the production data, is the only uncertain geological property. The reference log transformed permeability field, $\ln k$, used to generate the synthetic production data is shown in Fig. 7. The major feature of this reservoir is a high permeability streak crossing in the main flow direction. The reservoir is completed with a horizontal injector on the west side and a horizontal producer on the east side. Both the injector and the producer are composed of ten equal-length segments with control valves on every segment. The injection and production rate through each segment can be monitored and controlled. The control parameters in this case are the degree of opening of each control valve. The location of the valves are shown in Fig. 7 with triangles and half circles for the producer and the injector, respectively. They are numbered from one to ten.

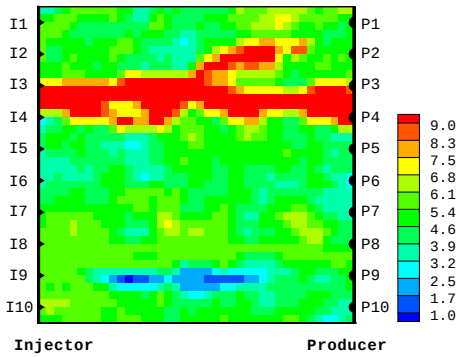

Figure 7: The reference $\ln k$ field, and the location of the control valves.

The horizontal injector is controlled by water injection rate of 4100 stb/day. The horizontal producer is controlled by bottom hole pressure of 2000 psi. The simulation lasts 1140 days that is roughly the period for injecting one pore volume of water based on the total injection rate constraint (4100 stb/day). The objective is to maximize the NPV by the end of 1140 days. The price of oil is \$70/bbl and the cost of water disposal is \$5/bbl. Zero discount rate is used in this example. The control settings are adjusted every two months, thus the number of control steps is 19 and the number of control parameters is 380. The production data available include water rate through each injector segment, oil and water production rates through each producer segment and the bottom hole pressure of the injector. These production data are assumed to be available at day 30, 90, 270 and 450. 60 realizations are used in this example.

Results and discussions We compare four different control scenarios in this example:

1. No-control: All the segments are fully open.
2. Reactive control: All the segments are fully open initially and the segments are subsequently closed according to the water oil ratio.
3. Optimization with known geology: The reservoir geological properties are assumed to be known without uncertainty and the production optimization is done based on the "true" reservoir.
4. Closed-loop optimization: The reservoir gridblock permeability is assumed to be uncertain. The EnKF is used to improve the estimation of the permeability. The valve settings are optimized under the uncertain reservoir description through the EnOpt.

The first two scenarios serve as base cases. The no-control case represents the situation where no control valves are available. The reactive control case changes the valve settings by merely reacting to the production responses from the true reservoir. It mimics the typical remedy taken in the field without the help of model-based optimization techniques. The third case, optimization with known geology represents the same situation as the previous example where the reservoir properties are assumed to be known. The optimization with known geology case serves as a reference, to which we can compare the results of the closed-loop optimization.

Closed-loop optimization with uncertain geology is the focus of this example. The EnKF updates the estimate of the permeability field and the EnOpt optimizes the valve settings based on the latest estimate of the permeability field. We could expect that if the closed-loop optimization did well, the NPV earned in the closed-loop optimization case should be similar to that earned in the case of optimization with known geology. In the closed-loop optimization, initially all the segments are fully open, and the production optimization starts after the assimilation of the first set of production data at day 30. The production optimization is repeated after each update of the geological model and the optimized control settings are expected to be more appropriate for the true reservoir with better prediction of the reservoir responses provided by the updated reservoir model.

Fig. 8 shows the mean of the initial $\ln k$ ensemble and the mean of the $\ln k$ ensemble updated at three different data times. The initial $\ln k$ realizations are generated using conditional sequential Gaussian simulation with hard data taken at the well locations on the west and east side. For lack of better information, the prior covariance is assumed to be isotropic with range equal to 800 ft. Data assimilation is influenced by the process of production optimization and becomes more complicated, since some extreme control settings, for example some valves being fully closed, make the geological feature of those regions not sensitive to the production data. We used iterations in addition to the traditional EnKF scheme to insure a good development of the geological feature based on limit production data available. Details of the iterative EnKF can be found in Gu and Oliver (2007). Out of the four data times, iterations were used for the assimilation of data at day 30, 270 and 450. Although using iterations increases the computational effort, a good estimate of the geological properties of the reservoir is beneficial to the production optimization and improves the entire closed-loop optimization process. As shown in Fig. 8, just after the assimilation of the first production data the feature of the high permeability streak is already clearly captured in the mean $\ln k$ field. With more information at the later data times, the connectivity of the high permeability streak is further improved and some secondary features of the reference field are also shown in the mean field, for example the low permeability and high permeability region in the south part of the reservoir, although not exactly identical to those in the reference field.

Fig. 9 compares the water saturation at day 1140, for the different scenarios. If all the segments are fully open, the no-control case, water breaks through along the high permeability streak very fast and leaves much oil behind after injecting one pore volume of water. In the reactive control case, the producer segments are gradually closed as the water cut increases. The producer segments near the high permeability streak are shut in at the late time, and this allows the injected water to better sweep the rest part of the reservoir. The final sweep efficiency of the reactive case is much higher than the no-control case. Both closed-loop optimization and optimization with known geology, however, show much higher sweep efficiency at day 1140 compared to the reactive case. By optimizing the NPV at the end of reservoir life we are able to adjust the control settings intelligently before the presence of water at the production side, while in the reactive case remedies can only be done after the water breakthrough, and the early detrimental behavior are not completely recoverable. For example, by gradually shutting in the producer segments near the high permeability streak after the water breakthrough the south part of the reservoir is better swept in the reactive case compared to the no-control case, but the residual oil saturation near the north boundary at day 1140 is similar to that of the no-control case because of the ready-formed easy flow path for the water.

Fig. 10 compares the water production rate of each segment of the producer between the reactive case and the optimized cases. The advantages of the model-based optimization technique can be more obviously seen in these plots. The water production are largely reduced after the presence of high water production in the reactive case by closing the corresponding control valves. The optimized cases can, however, prevent early water production by adjusting the setting of the control valves and eventually result in better sweep efficiency.

The field production profiles for these four cases are shown in Fig. 11. The top panel compares the oil and water production rate and the bottom panel compares the cumulative oil and water production for difference scenarios. The green curve indicates the no-control case, the blue curve indicates the reactive case, the black curve indicates the closed-loop optimization case and the red curve indicates the optimization with known geology case. The green and blue curve overlaps each other before the water breakthrough. After water breakthrough the reactive case shows higher oil production and lower water production compared to the no control case. The red and black curves exhibit very similar behavior, although the contribution from different segments are somewhat different between these two cases (as shown in Fig. 10). Both the closed-loop optimization case and the optimization with known

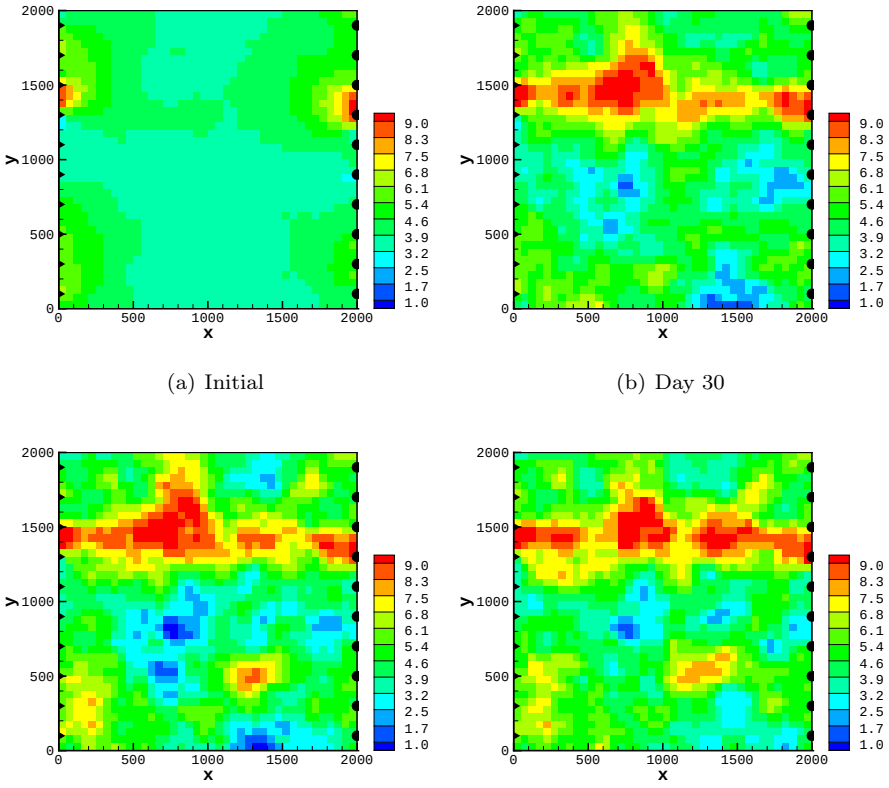

(a) Initial

(b) Day 30

(c) Day 90

(d) Day 450

Figure 8: Mean of the initial $\ln k$ ensemble and mean of $\ln k$ ensemble updated at three different data times.

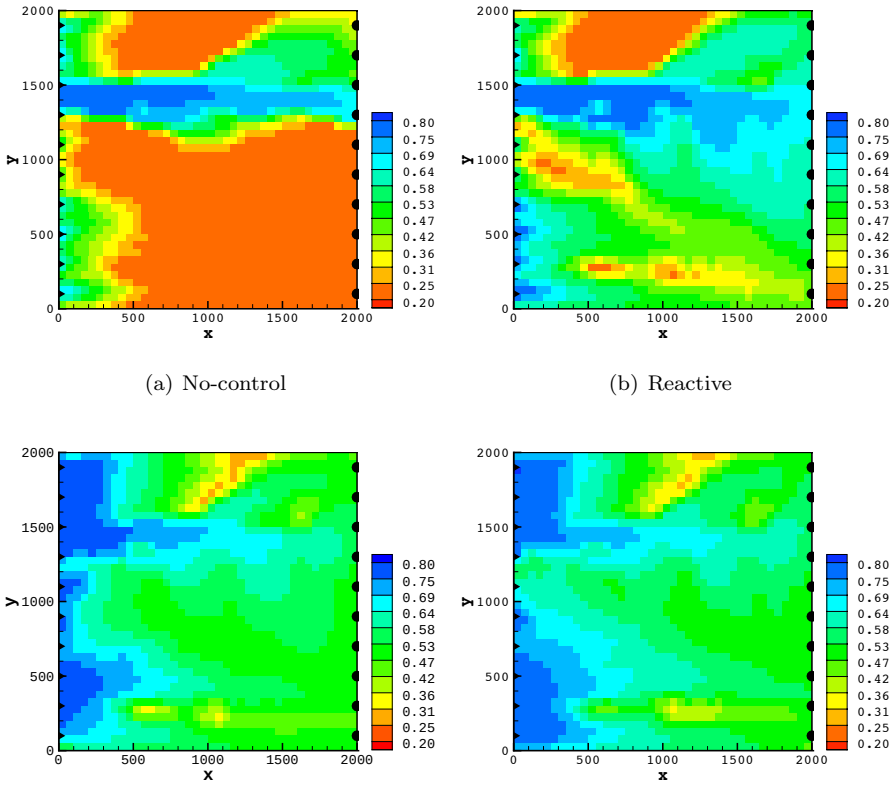

(a) No-control (b) Reactive

(c) Closed-loop (d) Opt with known geology

Figure 9: Water saturation at day 1140 for different scenarios.

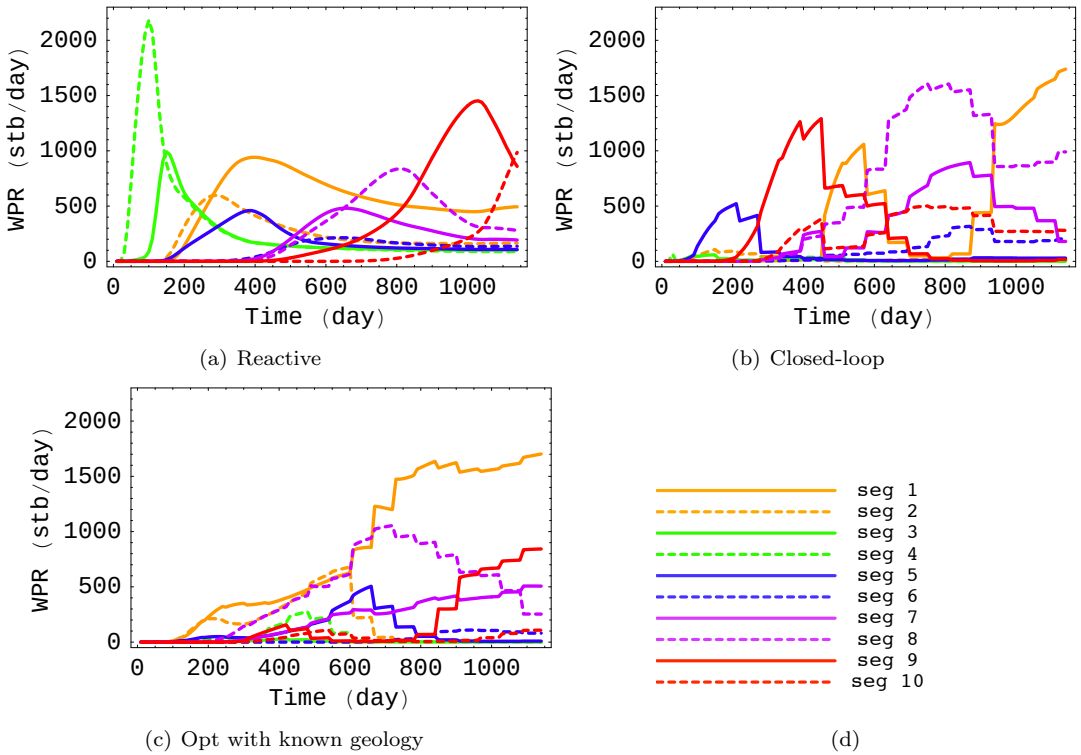

(a) Reactive (b) Closed-loop

(c) Opt with known geology (d)

Figure 10: Water production rate from each segment of the producer for different scenarios.

geology case show much higher oil production at early time. The optimized control settings at each data time vary in the closed-loop optimization since the optimization is performed based on the geological model updated at different data times, and the production profiles show some sudden changes at the data assimilation time due to the change of the well constraints. In general the closed-loop optimization performed well and the results are comparable with the case where the geological properties are assumed to be known.

The optimized control settings computed at subsequent data assimilation times result in a gradual increase in the NPV, if applied to the true field. But the amount of increase is not very large, because the high permeability streak feature of this reservoir is relatively simple and the main feature is captured by only incorporating the production data at the first data time. The NPV earned in the closed-loop optimization case is very close to that earned in the case of optimization with known geology, as seen by the similar cumulative oil and water production profiles in Fig. 11. The NPV is increased by 254% from the no control case and 22% from the reactive control case.

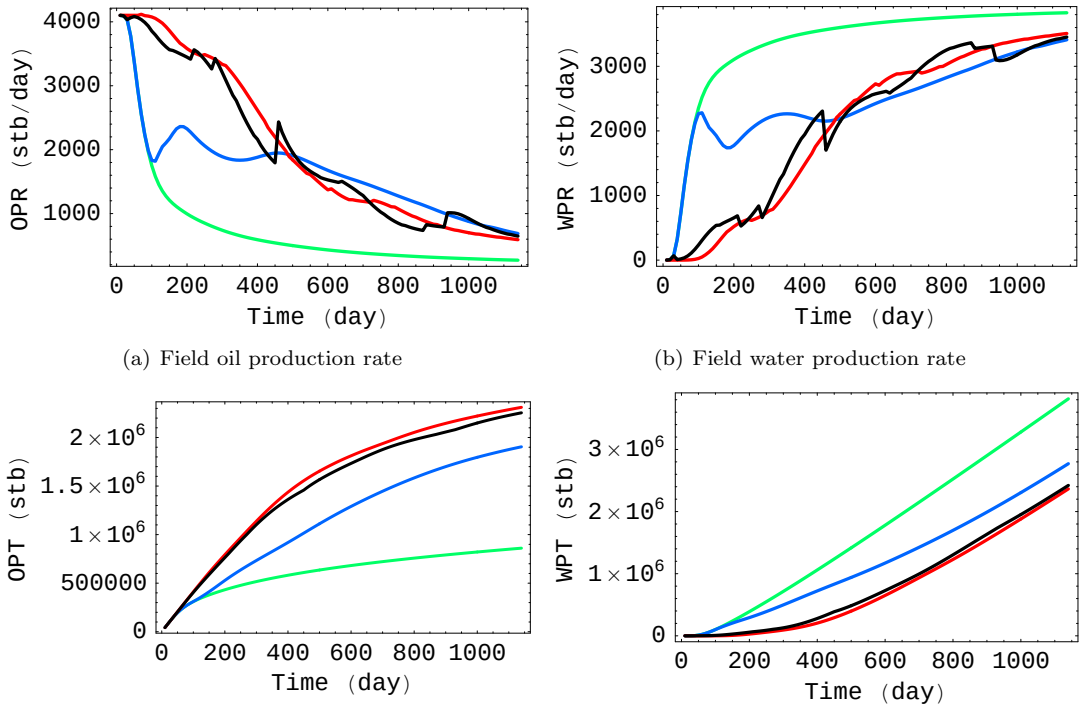

(a) Field oil production rate

(b) Field water production rate

(c) Cumulative oil production

(d) Cumulative water production

Figure 11: Comparison of the field production responses among different cases: no control (green); reactive (blue); closed-loop (black); optimization with known geology (red).

To show the quality of the estimate of the permeability field we compare the production responses using the optimized controls with the initial permeability ensemble and the permeability ensemble updated at day 450. Production responses from the initial reservoir ensemble are shown in Fig. 12 and the corresponding production responses from the ensemble updated at day 450 are shown in Fig. 13. The red curve indicates the reference production responses and the gray box plot shows the statistics from the ensemble forecast. The box contains 50% probability, the horizontal line in the box indicates the median and the whiskers indicate the maximum and the minimum values. It is obvious that the predictions based on the initial ensemble are very different from the reference production responses and show very high uncertainty, while the predictions from the updated permeability ensemble show better match to the data (production data at day 30, 90, 270 and 450) and better predictability. Note the data assimilation only utilized production data up to day 450, and no information from the rest of the production was used.

Conclusions

An ensemble-based closed-loop optimization is proposed in this paper. It combines the ensemble Kalman filter (EnKF) or an iterative method, the ensemble randomized maximum likelihood method (EnRML), with a new ensemble-based production optimization method (EnOpt). The EnKF has been used as an alternative to the

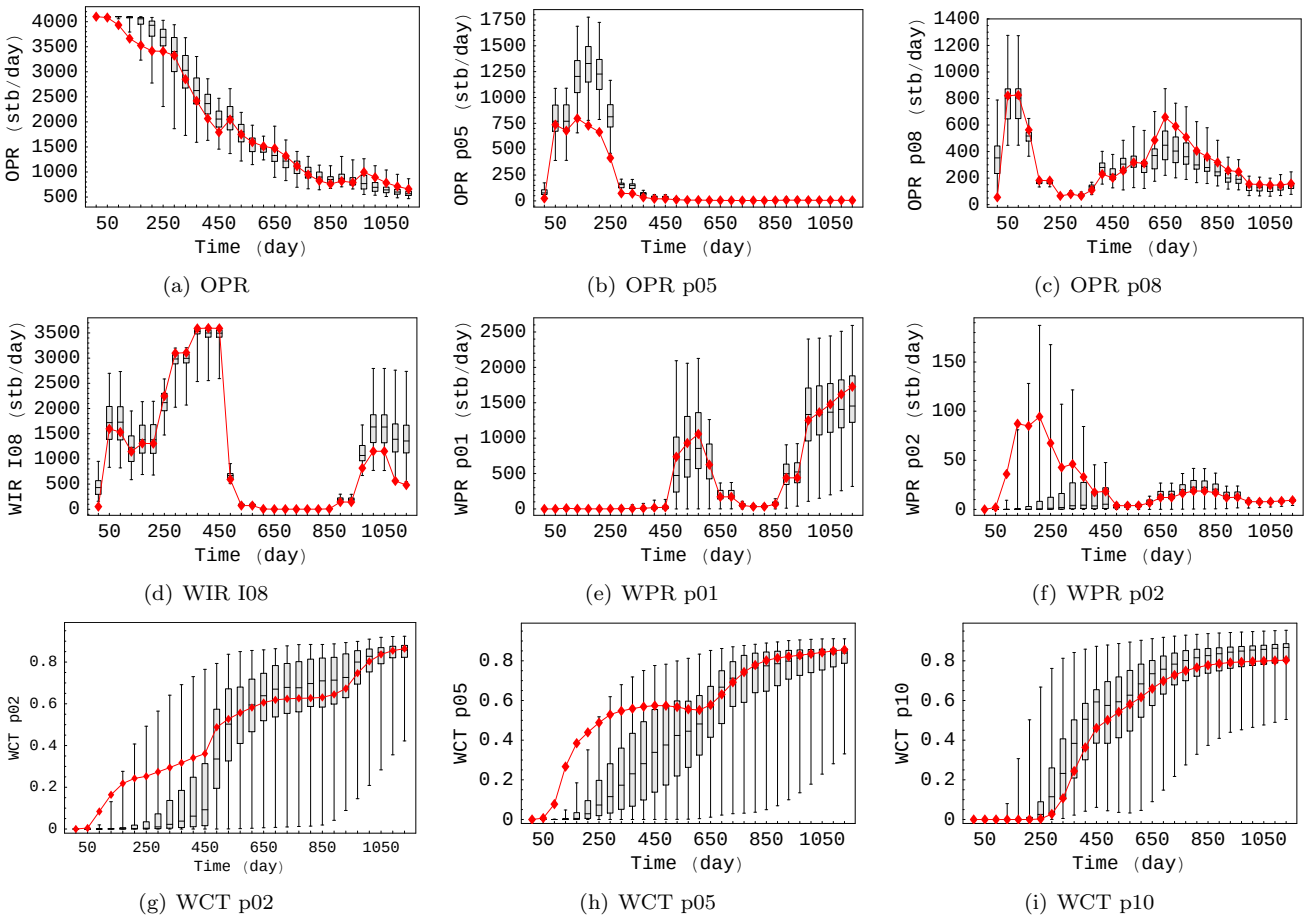

(a) OPR (b) OPR p05 (c) OPR p08

(d) WIR I08 (e) WPR p01 (f) WPR p02

(g) WCT p02 (h) WCT p05 (i) WCT p10

Figure 12: Data match from the initial ensemble.

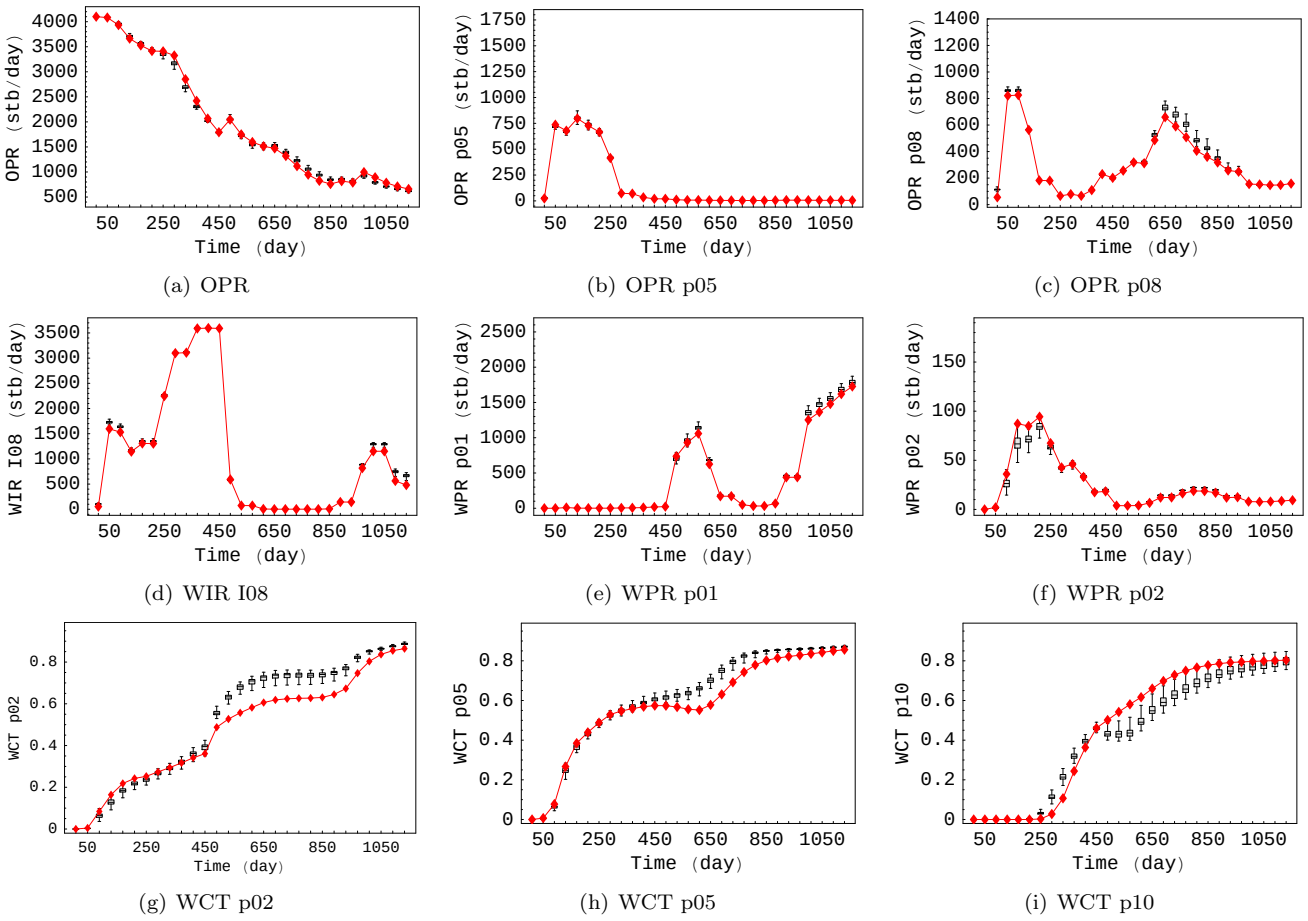

(a) OPR (b) OPR p05 (c) OPR p08

(d) WIR I08 (e) WPR p01 (f) WPR p02

(g) WCT p02 (h) WCT p05 (i) WCT p10

Figure 13: Data match from the ensemble updated at day 450.

traditional history matching method for several years and shown to be efficient and relatively robust. We found that it was sometimes beneficial to use the EnRML (Gu and Oliver, 2007) to improve the estimation of the uncertain geological properties. The EnOpt is used to adjust the production control variables to optimize the net present value over the uncertain reservoir description.

The sensitivities needed in the data assimilation and the production optimization are approximated from the ensemble in a very straightforward manner without the need for adjoint computation. The ensemble-based closed-loop optimization is very flexible since it is independent of the choice of the reservoir simulator and the financial model, thus it can be easily combined with any reservoir simulator and financial model with very limited amount of code development. The efficiency of this closed-loop optimization method results from the use of small ensembles of realizations for data assimilation and production optimization. The ensemble-based closed-loop optimization is also well suited to parallel computation. Based on current experience, 60 realizations appears to be enough for practical implementations. If necessary, the ensemble approximation can be further improved by intelligently selecting the initial ensemble and using localization to reduce the spurious correlation.

In the ensemble-based closed-loop optimization, we optimize the control variables with consideration of the uncertain description the geological properties. The uncertainty of the geological model is provided by the EnKF through an ensemble of plausible reservoir models. By choosing the expectation of the net present value to be the objective, the ensemble-based closed-loop optimization is fairly robust to uncertainty in reservoir description.

The applicability of the EnOpt and the ensemble-based closed-loop optimization is assessed through the use of two synthetic examples. In the first example, the well controls are optimized by the EnOpt based on a known channelized reservoir model. The results showed the ability of the EnOpt to improve reservoir management in the presence of complex geological features. The ensemble-based closed-loop optimization is demonstrated in the second example and the results are compared with other alternative control scenarios. A good estimate of the permeability field, which captured the main features of the reference field, was obtained through the EnRML. The net present value of the field is significantly increased by the closed-loop optimization and the level of increase is comparable with the hypothetical case where the optimization is performed with known geology.

Acknowledgment

We acknowledge the financial support of the member companies of the OU Consortium on Ensemble Methods. Multiple licenses of ECLIPSE were donated by Schlumberger. Computational resources were provided by the OU Supercomputing Center for Education and Research.

References

Agbalaka, C. C., Oliver, D. S., 2007. Application of the EnKF and localization to automatic history matching of facies distribution and production data. Math geology , accepted.

Arroyo-Negrete, E., Devegowda, D., Datta-Gupta, A., Choe, J., 2006. Streamline assisted ensemble Kalman filter for rapid and continuous reservoir model updating (SPE 104255). In: Proc. of the International Oil & Gas Conference and Exhibition in China, 5-7 December 2006, Beijing, China.

Bertino, L., Evensen, G., Wackernagel, H., 2003. Sequential data assimilation techniques in oceanography. International Statistical Review 71 (2), 223–241.

Brouwer, D. R., Nævdal, G., Jansen, J. D., Vefring, E. H., van Kruijsdijk, C. P. J. W., 2004. Improved reservoir management through optimal control and continuous model updating. In: SPE Annual Technical Conference and Exhibition, 26-29 September, Houston, Texas.

Burgers, G., van Leeuwen, P. J., Evensen, G., 1998. Analysis scheme in the ensemble Kalman filter. Monthly Weather Review 126, 1719–1724.

Chen, Y., Oliver, D. S., Zhang, D., 2007. Data assimilation for nonlinear problems by ensemble Kalman filter with reparameterization. Journal of Petroleum Science and Engineering , submitted.

Chen, Y., Zhang, D., 2006. Data assimilation for transient flow in geologic formations via ensemble Kalman filter. Advances in Water Resources 29 (8), 1107–1122.

Evensen, G., 1994. Sequential data assimilation with a nonlinear quasi-geostrophic model using Monte Carlo methods to forecast error statistics. Journal of Geophysical Research 99 (C5), 10143–10162.

Evensen, G., 2003. The ensemble Kalman filter: Theoretical formulation and practical implementation. Ocean Dynamics 53, 343–367.

Gu, Y., Oliver, D. S., 2005. History matching of the PUNQ-S3 reservoir model using the ensemble Kalman filter. SPE Journal 10 (2), 51–65.

Gu, Y., Oliver, D. S., 2007. An iterative ensemble Kalman filter for multiphase fluid flow data assimilation. SPE Journal 12 (4), 438–446.

Hamill, T. M., Whitaker, J. S., 2001. Distance-dependent filtering of background error covariance estimates in an ensemble Kalman filter. Monthly Weather Review 129 (11), 2776–2790.

Haugen, V., Natvik, L.-J., Evensen, G., Berg, A., Flornes, K., Nævdal, G., 2006. History matching using the ensemble Kalman filter on a North Sea field case (SPE-102430). In: SPE Annual Technical Conference and Exhibition.

Houtekamer, P. L., Mitchell, H. L., 2001. A sequential ensemble Kalman filter for atmospheric data assimilation. Monthly Weather Review 129 (1), 123–137.

Li, G., Reynolds, A., 2007. An iterative ensemble Kalman filter for data assimilation, SPE-109808. In: Proceeding of 2007 SPE Annual Technical Conference and Exhibition.

Li, R., Reynolds, A. C., Oliver, D. S., 2003. History matching of three-phase flow production data. SPE Journal 8 (4), 328–340.

Liu, N., Oliver, D. S., 2005. Ensemble Kalman filter for automatic history matching of geologic facies. Journal of Petroleum Science and Engineering 47 (3–4), 147–161.

Lorentzen, R. J., Berg, A. M., Nævdal, G., Vefring, E. H., 2006. A new approach for dynamic optimization of waterflooding problems, SPE-99690. In: Proceedings of the 2006 SPE intelligent energy conference and Exhibition.

Mitchell, H. L., Houtekamer, P. L., Pellerin, G., 2002. Ensemble size, balance, and model-error representation in an ensemble Kalman filter. Monthly Weather Review 130 (11), 2791–2808–433.

Nævdal, G., Johnsen, L. M., Aanonsen, S. I., Vefring, E. H., 2005. Reservoir monitoring and continuous model updating using ensemble Kalman filter. SPE Journal 10 (1), 66–74.

Oliver, D. S., 1995. Moving averages for Gaussian simulation in two and three dimensions. Mathematical Geology 27 (8), 939–960.

Sarma, P., Aziz, K., Durlofsky, L., 2005a. Implementation of adjoint solution for optimal control of smart wells, SPE-92864.

Sarma, P., Durlofsky, L., Aziz, K., 2005b. Efficient closed-loop production optimization under uncertainty, SPE-94241.

Tarantola, A., 2005. Inverse Problem Theory: Methods for Data Fitting and Model Parameter Estimation. Elsevier, Amsterdam, The Netherlands.

Van Doren, J. F. M., Van den Hof, P. M. J., Jansen, J. D., Bosgra, H., 2008. Determining identifiable parameterizations for large-scale physical models in reservoir engineering. In: Proceedings of the 17th Int. Fed. Autom. Control (IFAC) World Congress, Seoul, Korea, July 6–11.

van Essen, G., Zandvliet, M., van den Hof, P., Bosgra, O., Jansen, J., 2006. Robust waterflooding optimization of multiple geological scenario, SPE-102913. In: Proceedings of the 2006 SPE Annual Technical Conference and Exhibition.

Wang, C., Li, G., Reynolds, A. C., 2007. Production optimization in closed-loop reservoir management, SPE 109805. In: 2007 SPE Annual Technical Conference and Exhibition.